

Electron-phonon coupling and spin-charge separation in one-dimensional Mott insulators

H. Matsueda,^{1,*} T. Tohyama,^{1,†} and S. Maekawa^{1,2}

¹*Institute for Materials Research, Tohoku University, Sendai 980-8577, Japan*

²*CREST, Japan Science and Technology Agency (JST), Kawaguchi 332-0012, Japan*

(Received 8 November 2006; published 11 December 2006)

We examine the single-particle excitation spectrum in the one-dimensional Hubbard-Holstein model at half-filling by performing a dynamical density matrix renormalization group calculation. The spin-charge separation is robust against the electron-phonon (EP) coupling, although both spinon and holon branches are affected by phonons. We find that this robustness is in sharp contrast to a rather strong influence of the EP coupling on quasiparticle properties in two dimensions. We discuss the implication of the results of recent angle-resolved photoemission spectroscopy measurements on SrCuO₂.

DOI: [10.1103/PhysRevB.74.241103](https://doi.org/10.1103/PhysRevB.74.241103)

PACS number(s): 71.10.Fd, 71.38.-k, 79.60.-i, 74.72.Jt

In one-dimensional (1D) systems, the electron-phonon (EP) coupling represents one of the fundamental open problems. A well-known phenomenon is the Peierls instability. The instability significantly softens the phonon frequency in 1D, leading to charge-ordered states. Since the order is suppressed by the electron correlation, it is believed that the coupling does not play an important role in Mott insulators. However, in the doped Mott insulators, the EP coupling influences doped carriers propagating with charge fluctuation. Due to involved spin degrees of freedom, one now faces a problem different from the conventional polaron one. Furthermore, the electron correlation breaks an electron into collective modes representing spin and charge degrees of freedom, called spinons and holons, respectively.¹ Thus, the EP coupling may influence the spin-charge separation. In particular, a deeper understanding of the interdependence between the EP coupling and the spin-charge separation will be a guide for control of the internal degrees of freedom in real materials. Nevertheless, up to now, the spin-charge separation is the only key ingredient that provides nontrivial 1D physics. In this Rapid Communication, we provide insight into the interplay of the EP coupling and the spin-charge separation.

The EP coupling has been studied in 2D insulating cuprates. Angle-resolved photoemission spectroscopy (ARPES) experiments have revealed that the EP coupling leads to vanishing quasiparticle spectral weight.²⁻⁵ Since the quasiparticle is composed of spin and charge degrees of freedom, a comparison of our calculations with the 2D system will provide additional information on the influence of the EP coupling on the spin degrees of freedom.

We examine the single-particle excitation spectrum in the 1D Hubbard-Holstein (HH) model at half-filling. In the existing literature, there is only limited information on this spectrum, because the treatment of the electron correlation and the infinite number of photonic degrees of freedom on an equal footing represents a challenging problem.⁶⁻¹¹ In order to overcome this difficulty, we perform a large-scale dynamical density matrix renormalization group (DDMRG) calculation.

The calculation reveals that both spinon and holon singularities are smeared out. Particularly, in the strong-coupling regime, the phonon-charge (Holstein) coupling strongly affects the spinon as well as the holon branch. Nevertheless, we find that the spin-charge separation is robust against the

EP coupling, because the DDMRG results are well reproduced by performing a summation of the spectra for a spinless carrier dressed with phonons with different momenta. While the EP coupling does not affect the spin-charge separation in 1D, its effect on the spin degrees of freedom of the quasiparticle in 2D is much more pronounced.^{5,10,12} We discuss the implication of the results of recent ARPES measurements on SrCuO₂.

Let us introduce the Hamiltonian relevant for the insulating cuprates. The microscopic model includes Cu $3d_{x^2-y^2}$ and O $2p$ orbitals with lattice distortion. The highest occupied state is the Zhang-Rice singlet. We map the singlet and unoccupied $3d$ states onto the single-band Hubbard model. The distortion modulates the hopping integral of an electron between neighboring Cu and O orbitals. Due to the modulation, the diagonal (Holstein) electron-phonon coupling emerges in the single-band model, which is dominant in comparison with the off-diagonal (Peierls) coupling.^{13,14} Then, the Hamiltonian is defined by

$$H = -t \sum_{i,\sigma} (c_{i,\sigma}^\dagger c_{i+1,\sigma} + \text{H.c.}) + U \sum_i \left(n_{i,\uparrow} - \frac{1}{2} \right) \left(n_{i,\downarrow} - \frac{1}{2} \right) + \omega_0 \sum_i b_i^\dagger b_i - g \sum_i (b_i^\dagger + b_i)(n_i - 1), \quad (1)$$

where $c_{i,\sigma}^\dagger$ ($c_{i,\sigma}$) is the creation (annihilation) operator for an electron with spin σ at site i , b_i^\dagger (b_i) is the creation (annihilation) operator for an Einstein phonon at site i , $n_i = n_{i,\uparrow} + n_{i,\downarrow}$, $n_{i,\sigma} = c_{i,\sigma}^\dagger c_{i,\sigma}$, t is the hopping integral, U is the on-site Coulomb repulsion, ω_0 is the phonon frequency, and g is the EP coupling constant. We take U to be $U=8t$, which is an appropriate value for the cuprates.

We examine the single-particle excitation spectrum at zero temperature defined by

$$A(k, \omega) = -\frac{1}{\pi} \text{Im} \left\langle 0 \left| c_{k,\uparrow}^\dagger \frac{1}{E_0 - \omega - H + i\gamma} c_{k,\uparrow} \right| 0 \right\rangle, \quad (2)$$

where $c_{k,\uparrow}$ is the momentum representation of the electron operator $c_{i,\uparrow}$, $|0\rangle$ denotes the ground state with energy E_0 , and γ is a small positive number, which is taken to be $\gamma=0.1t$ in the present calculation.

Here, $A(k, \omega)$ is calculated by the finite-system DDMRG algorithm.¹⁵⁻²¹ The system size L is taken to be 20 lattice

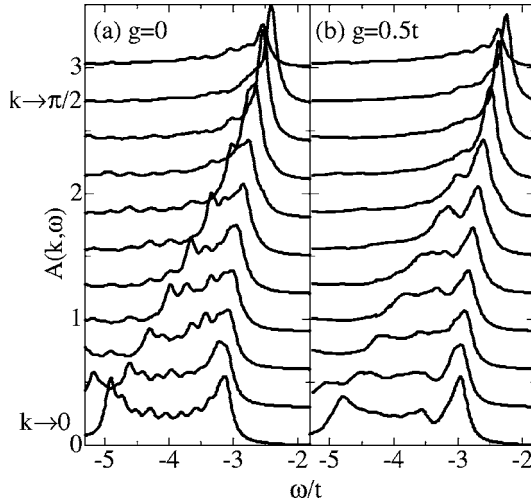


FIG. 1. $A(k, \omega)$ for the 1D Holstein-Hubbard model at half-filling. The momentum is taken from $\pi/21$ to $11\pi/21$.

sites. The DMRG bases are truncated up to $m=400$ states from the density matrix for a mixed state of the ground state $|0\rangle$, the final state after the one-electron-removal process $c_{k,\uparrow}|0\rangle$, and two correction vectors $(E_0 - \omega - H + i\gamma)^{-1}c_{k,\uparrow}|0\rangle$ for $\omega = \omega_1, \omega_2$ and $\omega_2 - \omega_1 = 2\gamma$. It is technically useful to note that convergent results are obtained when $A(k, \omega)$ and $A(k, \omega + 2\gamma)$ are smoothly connected for a given m .

In order to maintain numerical precision and reduce boundary effects, an open boundary condition is taken with potentials $-t_n$ at the edges. In such a system, the momentum k is defined by $k = n\pi/(L+1)$ with $n=1, 2, \dots, L$. The momentum representation of $c_{l,\uparrow}$ is given by $c_{k,\uparrow} = \sqrt{2/(L+1)} \sum_l \sin(kl) c_{l,\uparrow}$.^{19,20} It is noted that the spectrum for $L=20$ presented here is similar to that for $L=120$ without the edge potential.²⁰

In the DMRG calculation, phononic degrees of freedom at each site are truncated up to $M=2^N$ and then exactly transformed into a set of N hard-core bosons.²² The bosonic and electronic degrees of freedom are treated as different “sites.” Here, the maximum number of N which we take is 4 and the superblock is composed of $(1+N)L=100$ sites. This transformation enables us to calculate the spectra for large values of g . However, the highest-order boson is renormalized at first in some processes, which worsens the numerical precision. Thus, we set up superblocks so that the final sweep process keeps the precision.

Figure 1 shows $A(k, \omega)$ with and without the electron-phonon coupling g . The phonon frequency is taken to be $\omega_0 = 0.5t > \gamma = 0.1t$ in order to see the effect of the phonon clearly. While its value relevant for the cuprates is $\omega_0 \geq \gamma$, we have confirmed that our conclusion does not change for ω_0 as low as $\omega_0 = 0.2t$. The origin of the energy is located at the center of the Mott gap. In Fig. 1(a), two branches disperse, merging toward $k \rightarrow \pi/2$. These energy positions are $\omega/t = -3.13$ and -4.90 at $k = \pi/21$, which is the minimum momentum in the calculation. The branch located in the low-(high-) binding-energy side is deduced to be the spinon (holon) branch. Here, fine structures inside the branches come from a finite-size effect. It is noted that the bandwidth of the

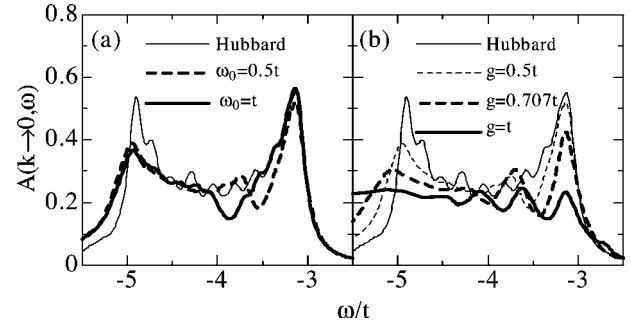


FIG. 2. (a) $A(k \rightarrow 0, \omega)$ for various ω_0 values. For $\omega_0 \neq 0$, g is taken to be $0.5t$. (b) $A(k \rightarrow 0, \omega)$ with $\omega_0 = 0.5t$ for various g values. For (a) and (b), the spectra with $g \neq 0$ are shifted so that the energy of the spinon branch is taken to be equal.

holon branch from $k = \pi/21$ to $k = 10\pi/21$ depends on the open boundary condition and U . In Fig. 1(b), we find that the holon branch broadens due to the EP coupling, while the spinon branch remains sharp. We also identify a “peak-dip-hump” structure at the high-binding-energy side of the spinon branch. The dip disperses like the spinon branch. As shown in Fig. 2(a), the energy of the dip (hump) position decreases with increasing ω_0 . The energy difference between the dip (hump) and the spinon branch is estimated to be ω_0 , which means that the peak-dip-hump structure emerges due to the EP coupling. Therefore, the shape of the peak-dip-hump structure provides information on the phonon frequency.

As g increases beyond $0.5t$ while keeping $\omega_0 = 0.5t$, the spinon branch starts to broaden.⁷ In Fig. 2(b), we show $A(k \rightarrow 0, \omega)$ for various g values. The weight of the spinon branch decreases linearly as a function of g for $g \geq \omega_0$. For $g = t$, the holon branch is completely smeared out. The peak-dip-hump structure observed in Fig. 1(b) develops into multiple peaks positioned at $\omega/t = -3.13$, -3.61 to $-3.13 - \omega_0$, and -4.09 to $-3.13 - 2\omega_0$, respectively. Furthermore, a slight enhancement of the low-binding energy side of the spinon branch is seen. The energy difference between the enhancement and the band top ($k = \pi/2$) for $g = 0$ is estimated to be ω_0 . Therefore, the three main peaks and the enhancement are also due to the EP coupling.

As mentioned in the previous two paragraphs, the following phonon effects appear on $A(k, \omega)$: (i) a peak-dip-hump structure, (ii) a broad holon branch, (iii) a decrease of the spectral weight of the spinon branch, and (iv) an enhancement of the low-binding-energy side of the spinon branch. In particular, the characteristic energy scale of (i) and (iv) is ω_0 . In light of the spin-charge separation, they can be interpreted as follows.

First, we consider the origins of (i) and (ii) shown in Fig. 1(b) for $g = 0.5t = \omega_0$. Let us start with the dispersion in the Hubbard model as illustrated in Fig. 3(a). According to the Bethe ansatz solution, the dispersion is constructed by a superposition of a set of holon dispersions forming a cosine band with width $4t$.²³ The superposition is a consequence of the spin-charge separation, because each of the holon dispersions is characterized by one spinon momentum. Therefore, an effective model of $A(k, \omega)$, $A_{\text{eff}}(k, \omega)$, is constructed by putting the spectral weight for a spinless fermion, $A_h(p, \varepsilon)$

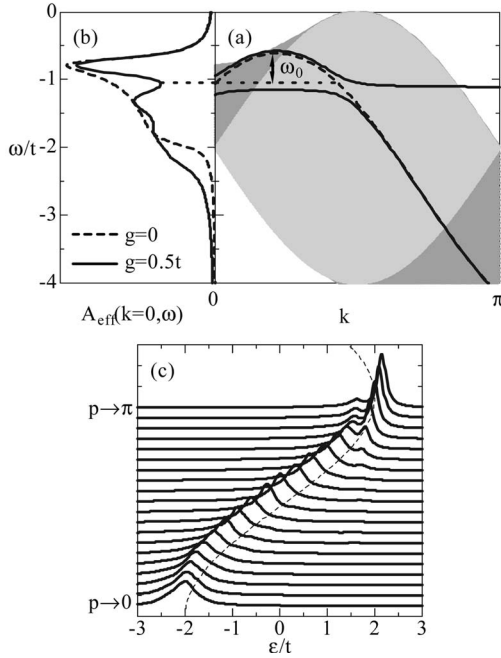


FIG. 3. (a) Shaded area: schematic view of the dispersion in a 1D Mott insulator, dashed (solid) line: one holon dispersion for $g=0$ ($g \neq 0$). The dotted line is a guide to the eye. (b) $A_{\text{eff}}(k=0, \omega)$, dashed (solid) line: $g=0$ ($g=\omega_0=0.5t$). Here, the broadening γ is assumed. (c) $A_h(p-\pi, \varepsilon)$ for the 1D Holstein model—i.e. a model for a spinless carrier with Einstein phonons ($g=\omega_0=0.5t$). The dashed line represents a cosine band with width $4t$.

$=\delta(\varepsilon-2t \cos p)$, on each of the holon dispersions. Since the top of the cosine band is running along the spinon dispersion $\varepsilon_s(q+\pi/2)=-\pi J/2|\sin(q+\pi/2)|$ for $-\pi/2 \leq q \leq \pi/2$, $A_{\text{eff}}(k, \omega)$ is defined by

$$A_{\text{eff}}(k, \omega) = \sum_{q=-\pi/2}^{\pi/2} A_h\left(k-q, \omega+2t+\varepsilon_s\left(q+\frac{\pi}{2}\right)\right), \quad (3)$$

apart from a constant energy shift. A dashed line in Fig. 3(b) shows $A_{\text{eff}}(k=0, \omega)$. The singularity of the spinon branch appears at $\omega=-\pi J/2 \sim -2\pi t^2/U=-0.785t$ and in the flat part of the spinon dispersion near $k=0$. The line shape is consistent with the DDMRG data in Fig. 1(a) except for the singularity of the holon branch. The singularity of the holon branch is recovered from the phase string effect.²⁴ The consistency indicates that Eq. (3) is appropriate for the spectral weight in spin-charge-separated systems.

Let us introduce the EP coupling and take g to be $0.5t$. Due to the spin-charge separation, each of the holons couples with phonons independently. Namely, $A_h(p, \varepsilon)$ is given by the spectra for a spinless carrier dressed with Einstein phonons. Figure 3(c) shows $A_h(p-\pi, \varepsilon)$, which splits into low-lying peaks and an incoherent part.^{25–28} The split occurs at the anticrossing point $\varepsilon \sim 1.5t$ shifted from the top of the band ($p=\pi$) by ω_0 . At $\varepsilon \sim 1.5t$, we find a tiny spectral weight with a flat dispersion coming from the phonon branch. In Fig. 3(a), the split of one holon dispersion is illustrated. $A_{\text{eff}}(k=0, \omega)$ is then given by the solid line in Fig. 3(b). A peak-dip-hump structure appears. The spectral weight lost by

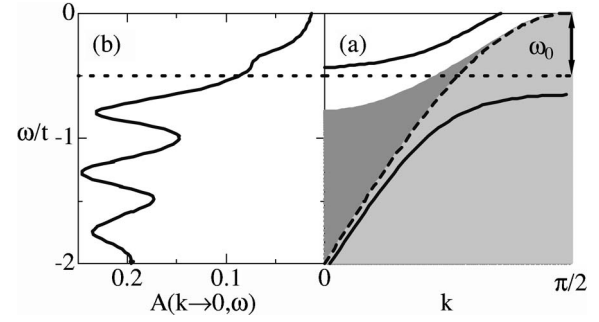


FIG. 4. (a) Shaded area: schematic view of the dispersion in a 1D Mott insulator, dashed (solid) line: one holon dispersion for $g=0$ ($g \neq 0$). The dotted line is a guide to the eye. (b) $A(k \rightarrow 0, \omega)$ for $g=t$ and $\omega_0=0.5t$.

the dip is transferred to the high-energy region. The spinon branch, the dip, and the broad holon branch originate from the low-lying peak, the anticrossing, and the incoherent part of $A_h(p, \varepsilon)$, respectively. These features obtained by Eq. (3) are consistent with the DDMRG data, and thus the spin-charge separation is robust.

Next, we consider the origin of (iii) shown in Fig. 2(b) for $g \geq \omega_0$. As mentioned in the previous paragraph, the spinon branch can be expressed by the superposition of the low-lying peak in Fig. 3(c). It has been shown that the spectral weight of the low-lying peak decreases with increasing g .^{25–28} Therefore, the weight of the spinon branch decreases with increasing g .

Finally, the origin of (iv) is considered. In Fig. 4, we see that the small enhancement of the spectral weight on the low-binding-energy side comes from the phonon branch. Even for the coupling $g=t > \omega_0$, the spectral weight of the phonon branch is very weak at $k \sim 0$.^{25–28} This is the origin of the tiny weight seen in the DDMRG data. We should stress that the tiny weight is seen under the condition $\omega_0 < \pi J/2$.

All of our interpretations for (i)–(iv) show the robustness of the spin-charge separation against the EP coupling in the 1D HH model. The robustness is in contrast to the rather strong influence of the EP coupling on the spin degrees of freedom of the quasiparticle in 2D. In order to illustrate the difference, we introduce a dimensionless parameter $\lambda = g^2/\omega_0 W$ with the noninteracting bandwidth W . There exists a characteristic λ value—e.g., λ^* .²⁹ For $\lambda < \lambda^*$, the lowest-energy excitation is only weakly dressed with phonons. As λ approaches λ^* , the excitation rapidly loses its spectral weight, and then the weight flows into the phonon branches. In the 1D Holstein model, λ^* is estimated to be $\lambda^* \sim 1$.^{30,31} In the 1D HH model, the spinon branch loses its weight for $\lambda^* \sim 1$ ($g^* \sim 1.4t$) as estimated from Fig. 2(b).⁷ This is because the spinon branch can be expressed by superposition of the spectra for the low-energy excitation of the Holstein model. In 2D, on the other hand, λ^* is close to 0.2 in the t - J Holstein model with $J=0.3t$, while $\lambda^* > 0.6$ in the Holstein model.^{5,10,12} This means that the antiferromagnetic (AF) correlation facilitates the formation of the lattice polaron.^{32–34} As J increases, the energy gain originating in the AF correlation leads to the suppression of the coherent hole motion which in turn leads to the formation of the lattice polaron.

Finally, let us discuss the ARPES data for a 1D Mott insulator SrCuO₂ in light of the DDMRG results. In this compound, high-energy ARPES experiments have been performed, where the spinon and holon branches were observed.³⁵ Near the Γ point, the intensity of the holon branch is smaller than that of the spinon branch. In addition, these branches do not exhibit singularities predicted by the Hubbard model.²³ In Fig. 2(b), we show the DDMRG data for $\lambda=0.25$ ($g=0.707t$ and $\omega_0=0.5t$) that are appropriate for 1D cuprates.¹⁴ The DDMRG data are consistent with the ARPES data except for the missing dip. The dip may be washed away either by the phonon dispersion or smeared out due to finite-temperature effects.

In summary, we have examined the single-particle excitation spectrum in the 1D HH model at half-filling by performing a DDMRG calculation. The following are characteristic features in the spectrum: (i) a dip at the high-binding energy side of the spinon branch, (ii) broad holon branch, (iii) decrease of the spectral weight of the spinon branch, and (iv) slight enhancement of the weight at the low-binding-energy

side of the spinon branch. These results were well reproduced by performing a superposition of the spectra for a spinless carrier dressed with phonons. This means that the spin-charge separation is robust against the electron-phonon coupling. The spin degrees of freedom are not affected by the relatively strong EP coupling in 1D, while, in contrast, the AF correlation enhances the effect of the EP coupling in 2D. The ARPES data for SrCuO₂ were consistent with our DDMRG data.

Recently, it has come to our attention that the effect of the EP coupling on the single-particle excitation spectrum in 1D was studied in Ref. 11.

We thank P. Prelovšek for discussions and for giving us a copy of his work prior to publication. Helpful comments of J. Bonča on the manuscript are also acknowledged. This work was supported by the NAREGI Nanoscience Project and Grant-in-Aid for Scientific Research from the Ministry of Education, Culture, Sports, Science and Technology of Japan and CREST.

*Present address: Department of Physics, Tohoku University, Sendai 980-8578, Japan. Electronic address: matsueda@cmppt.phys.tohoku.ac.jp

†Present address: Yukawa Institute for Theoretical Physics, Kyoto University, Kyoto 606-8502, Japan.

¹C. Kim, A. Y. Matsuura, Z. X. Shen, N. Motoyama, H. Eisaki, S. Uchida, T. Tohyama, and S. Maekawa, Phys. Rev. Lett. **77**, 4054 (1996); C. Kim, Z. X. Shen, N. Motoyama, H. Eisaki, S. Uchida, T. Tohyama, and S. Maekawa, Phys. Rev. B **56**, 15589 (1997).

²A. Damascelli, Z. Hussain, and Z.-X. Shen, Rev. Mod. Phys. **75**, 473 (2003).

³K. M. Shen, F. Ronning, D. H. Lu, W. S. Lee, N. J. C. Ingle, W. Meevasana, F. Baumberger, A. Damascelli, N. P. Armitage, L. L. Miller, Y. Kohsaka, M. Azuma, M. Takano, H. Takagi, and Z.-X. Shen, Phys. Rev. Lett. **93**, 267002 (2004).

⁴O. Rösch, O. Gunnarsson, X. J. Zhou, T. Yoshida, T. Sasagawa, A. Fujimori, Z. Hussain, Z.-X. Shen, and S. Uchida, Phys. Rev. Lett. **95**, 227002 (2005).

⁵A. S. Mishchenko and N. Nagaosa, Phys. Rev. Lett. **93**, 036402 (2004).

⁶K. Tsutsui, T. Tohyama, and S. Maekawa, Physica C **392-396**, 199 (2003); J. Low Temp. Phys. **131**, 257 (2003).

⁷M. Capone, M. Grilli, and W. Stephan, Eur. Phys. J. B **11**, 551 (1999).

⁸M. Hohenadler, M. Aichhorn, and W. von der Linden, Phys. Rev. B **71**, 014302 (2005).

⁹H. Fehske, G. Wellein, G. Hager, A. Weiße, and A. R. Bishop, Phys. Rev. B **69**, 165115 (2004).

¹⁰B. Bäuml, G. Wellein, and H. Fehske, Phys. Rev. B **58**, 3663 (1998).

¹¹W.-Q. Ning, H. Zhao, C.-Q. Wu, and H.-Q. Lin, Phys. Rev. Lett. **96**, 156402 (2006).

¹²P. Prelovšek, R. Zeyher, and P. Horsch, Phys. Rev. Lett. **96**, 086402 (2006).

¹³G. Khaliullin and P. Horsch, Physica C **282-287**, 1751 (1997); P. Horsch and G. Khaliullin, Physica B **359-361**, 620 (2005); P. Horsch, G. Khaliullin, and V. Oudovenko, Physica C **341-348**,

117 (2000).

¹⁴O. Rösch and O. Gunnarsson, Phys. Rev. Lett. **92**, 146403 (2004); Phys. Rev. B **70**, 224518 (2004).

¹⁵S. R. White, Phys. Rev. Lett. **69**, 2863 (1992); Phys. Rev. B **48**, 10345 (1993).

¹⁶K. A. Hallberg, Phys. Rev. B **52**, R9827 (1995).

¹⁷T. D. Kühner and S. R. White, Phys. Rev. B **60**, 335 (1999).

¹⁸E. Jeckelmann, Phys. Rev. B **66**, 045114 (2002).

¹⁹H. Benthien, F. Gebhard, and E. Jeckelmann, Phys. Rev. Lett. **92**, 256401 (2004).

²⁰H. Matsueda, N. Bulut, T. Tohyama, and S. Maekawa, Phys. Rev. B **72**, 075136 (2005).

²¹N. Shibata, J. Phys. A **36**, R381 (2003).

²²E. Jeckelmann and S. R. White, Phys. Rev. B **57**, 6376 (1998).

²³A. Parola and S. Sorella, Phys. Rev. B **45**, R13156 (1992); S. Sorella and A. Parola, J. Phys.: Condens. Matter **4**, 3589 (1992).

²⁴H. Suzuura and N. Nagaosa, Phys. Rev. B **56**, 3548 (1997).

²⁵C. Zhang, E. Jeckelmann, and S. R. White, Phys. Rev. B **60**, 14092 (1999).

²⁶M. Hohenadler, M. Aichhorn, and W. von der Linden, Phys. Rev. B **68**, 184304 (2003).

²⁷S. Sykora, A. Hübsch, K. W. Becker, G. Wellein, and H. Fehske, Phys. Rev. B **71**, 045112 (2005).

²⁸H. Zhao, C.-Q. Wu, and H.-Q. Lin, Phys. Rev. B **71**, 115201 (2005).

²⁹V. V. Kabanov and O. Yu. Mashtakov, Phys. Rev. B **47**, 6060 (1993).

³⁰J. Bonča, S. A. Trugman, and I. Batistić, Phys. Rev. B **60**, 1633 (1999).

³¹G. Wellein and H. Fehske, Phys. Rev. B **56**, 4513 (1997).

³²E. Cappelluti and S. Ciuchi, Phys. Rev. B **66**, 165102 (2002).

³³G. Wellein, H. Röder, and H. Fehske, Phys. Rev. B **53**, 9666 (1996).

³⁴A. Ramšak, P. Horsch, and P. Fulde, Phys. Rev. B **46**, R14305 (1992).

³⁵B. J. Kim, H. Koh, E. Rotenberg, S.-J. Oh, H. Eisaki, N. Motoyama, S. Uchida, T. Tohyama, S. Maekawa, Z.-X. Shen, and C. Kim, Nat. Phys. **2**, 397 (2006).